



Queensland University of Technology
Brisbane Australia

This is the author's version of a work that was submitted/accepted for publication in the following source:

Rath, Subha Narayan, Prymachuk, Galyna, Bleiziffer, Oliver A., Lam, Christopher X.F., Arkudas, Andreas, Ho, Saey T. B., Beier, Justus P., Horch, Raymund E., [Hutmacher, Dietmar W.](#), & Kneser, Ulrich (2011) Hylaluronan-based heparin-incorporated hydrogels for generation of axially vascularized bioartificial bone tissues : in vitro and in vivo evaluation in a PLDLLA-TCP-PCL-composite system. *Journal of Materials Science : Materials in Medicine*.

This file was downloaded from: <http://eprints.qut.edu.au/41459/>

© Copyright 2011 Springer Science+Business Media, LLC

The original publication is available at SpringerLink
<http://www.springerlink.com>

Notice: *Changes introduced as a result of publishing processes such as copy-editing and formatting may not be reflected in this document. For a definitive version of this work, please refer to the published source:*

<http://dx.doi.org/10.1007/s10856-011-4300-0>

Dear Author,

Here are the proofs of your article.

- You can submit your corrections **online**, via **e-mail** or by **fax**.
- For **online** submission please insert your corrections in the online correction form. Always indicate the line number to which the correction refers.
- You can also insert your corrections in the proof PDF and **email** the annotated PDF.
- For fax submission, please ensure that your corrections are clearly legible. Use a fine black pen and write the correction in the margin, not too close to the edge of the page.
- Remember to note the **journal title**, **article number**, and **your name** when sending your response via e-mail or fax.
- **Check** the metadata sheet to make sure that the header information, especially author names and the corresponding affiliations are correctly shown.
- **Check** the questions that may have arisen during copy editing and insert your answers/ corrections.
- **Check** that the text is complete and that all figures, tables and their legends are included. Also check the accuracy of special characters, equations, and electronic supplementary material if applicable. If necessary refer to the *Edited manuscript*.
- The publication of inaccurate data such as dosages and units can have serious consequences. Please take particular care that all such details are correct.
- Please **do not** make changes that involve only matters of style. We have generally introduced forms that follow the journal's style. Substantial changes in content, e.g., new results, corrected values, title and authorship are not allowed without the approval of the responsible editor. In such a case, please contact the Editorial Office and return his/her consent together with the proof.
- If we do not receive your corrections **within 48 hours**, we will send you a reminder.
- Your article will be published **Online First** approximately one week after receipt of your corrected proofs. This is the **official first publication** citable with the DOI. **Further changes are, therefore, not possible.**
- The **printed version** will follow in a forthcoming issue.

Please note

After online publication, subscribers (personal/institutional) to this journal will have access to the complete article via the DOI using the URL: [http://dx.doi.org/\[DOI\]](http://dx.doi.org/[DOI]).

If you would like to know when your article has been published online, take advantage of our free alert service. For registration and further information go to: <http://www.springerlink.com>.

Due to the electronic nature of the procedure, the manuscript and the original figures will only be returned to you on special request. When you return your corrections, please inform us if you would like to have these documents returned.

Metadata of the article that will be visualized in OnlineFirst

Please note: Images will appear in color online but will be printed in black and white.

ArticleTitle Hyaluronan-based heparin-incorporated hydrogels for generation of axially vascularized bioartificial bone tissues: in vitro and in vivo evaluation in a PLDLLA–TCP–PCL-composite system

Article Sub-Title

Article CopyRight Springer Science+Business Media, LLC
(This will be the copyright line in the final PDF)

Journal Name Journal of Materials Science: Materials in Medicine

Corresponding Author

Family Name	Kneser
Particle	
Given Name	Ulrich
Suffix	
Division	Department of Plastic and Hand Surgery
Organization	University of Erlangen Medical Center
Address	Krankenhausstrasse 12, 91054, Erlangen, Germany
Email	Ulrich.kneser@uk-erlangen.de

Author

Family Name	Rath
Particle	
Given Name	Subha N.
Suffix	
Division	Department of Plastic and Hand Surgery
Organization	University of Erlangen Medical Center
Address	Krankenhausstrasse 12, 91054, Erlangen, Germany
Division	Division of Bioengineering
Organization	National University of Singapore
Address	21 Lower Kent Ridge Road, 119077, Singapore, Singapore
Email	

Author

Family Name	Prymachuk
Particle	
Given Name	Galyna
Suffix	
Division	Department of Plastic and Hand Surgery
Organization	University of Erlangen Medical Center
Address	Krankenhausstrasse 12, 91054, Erlangen, Germany
Email	

Author

Family Name	Bleiziffer
Particle	
Given Name	Oliver A.
Suffix	
Division	Department of Plastic and Hand Surgery
Organization	University of Erlangen Medical Center
Address	Krankenhausstrasse 12, 91054, Erlangen, Germany
Email	

Author	Family Name	Lam
	Particle	
	Given Name	Christopher X. F.
	Suffix	
	Division	Division of Bioengineering
	Organization	National University of Singapore
	Address	21 Lower Kent Ridge Road, 119077, Singapore, Singapore
	Email	
Author	Family Name	Arkudas
	Particle	
	Given Name	Andreas
	Suffix	
	Division	Department of Plastic and Hand Surgery
	Organization	University of Erlangen Medical Center
	Address	Krankenhausstrasse 12, 91054, Erlangen, Germany
	Email	
Author	Family Name	Ho
	Particle	
	Given Name	Saey T. B.
	Suffix	
	Division	Graduate Programme in Bioengineering, Yong Loo Lin School of Medicine
	Organization	National University of Singapore
	Address	28 Medical Drive, 117456, Singapore, Singapore
	Email	
Author	Family Name	Beier
	Particle	
	Given Name	Justus P.
	Suffix	
	Division	Department of Plastic and Hand Surgery
	Organization	University of Erlangen Medical Center
	Address	Krankenhausstrasse 12, 91054, Erlangen, Germany
	Email	
Author	Family Name	Horch
	Particle	
	Given Name	Raymund E.
	Suffix	
	Division	Department of Plastic and Hand Surgery
	Organization	University of Erlangen Medical Center
	Address	Krankenhausstrasse 12, 91054, Erlangen, Germany
	Email	
Author	Family Name	Hutmacher
	Particle	
	Given Name	Dietmar W.
	Suffix	

Division	Faculty of Engineering, Faculty of Science, Institute of Health and Biomedical Innovation
Organization	Queensland University of Technology
Address	4000, Brisbane, QLD, Australia
Email	

Schedule	Received	4 November 2010
	Revised	
	Accepted	16 March 2011

Abstract

Smart matrices are required in bone tissue-engineered grafts that provide an optimal environment for cells and retain osteo-inductive factors for sustained biological activity. We hypothesized that a slow-degrading heparin-incorporated hyaluronan (HA) hydrogel can preserve BMP-2; while an arterio-venous (A-V) loop can support axial vascularization to provide nutrition for a bio-artificial bone graft. HA was evaluated for osteoblast growth and BMP-2 release. Porous PLDLLA-TCP-PCL scaffolds were produced by rapid prototyping technology and applied in vivo along with HA-hydrogel, loaded with either primary osteoblasts or BMP-2. A microsurgically created A-V loop was placed around the scaffold, encased in an isolation chamber in Lewis rats. HA-hydrogel supported growth of osteoblasts over 8 weeks and allowed sustained release of BMP-2 over 35 days. The A-V loop provided an angiogenic stimulus with the formation of vascularized tissue in the scaffolds. Bone-specific genes were detected by real time RT-PCR after 8 weeks. However, no significant amount of bone was observed histologically. The heterotopic isolation chamber in combination with absent biomechanical stimulation might explain the insufficient bone formation despite adequate expression of bone-related genes. Optimization of the interplay of osteogenic cells and osteo-inductive factors might eventually generate sufficient amounts of axially vascularized bone grafts for reconstructive surgery.

Footnote Information

3 Hyaluronan-based heparin-incorporated hydrogels for generation 4 of axially vascularized bioartificial bone tissues: in vitro 5 and in vivo evaluation in a PLDLLA–TCP–PCL- 6 composite system

7 Subha N. Rath · Galyna Prymachuk · Oliver A. Bleiziffer · Christopher X. F. Lam ·
8 Andreas Arkudas · Saey T. B. Ho · Justus P. Beier · Raymund E. Horch ·
9 Dietmar W. Hutmacher · Ulrich Kneser

10 Received: 4 November 2010 / Accepted: 16 March 2011
11 © Springer Science+Business Media, LLC 2011

13 **Abstract** Smart matrices are required in bone tissue-
14 engineered grafts that provide an optimal environment for
15 cells and retain osteo-inductive factors for sustained bio-
16 logical activity. We hypothesized that a slow-degrading
17 heparin-incorporated hyaluronan (HA) hydrogel can pre-
18 serve BMP-2; while an arterio–venous (A–V) loop can
19 support axial vascularization to provide nutrition for a bio-
20 artificial bone graft. HA was evaluated for osteoblast
21 growth and BMP-2 release. Porous PLDLLA–TCP–PCL
22 scaffolds were produced by rapid prototyping technology
23 and applied in vivo along with HA-hydrogel, loaded with
24 either primary osteoblasts or BMP-2. A microsurgically
25 created A–V loop was placed around the scaffold, encased
26 in an isolation chamber in Lewis rats. HA-hydrogel sup-
27 ported growth of osteoblasts over 8 weeks and allowed
28 sustained release of BMP-2 over 35 days. The A–V loop

provided an angiogenic stimulus with the formation of 29
vascularized tissue in the scaffolds. Bone-specific genes 30
were detected by real time RT-PCR after 8 weeks. 31
However, no significant amount of bone was observed 32
histologically. The heterotopic isolation chamber in com- 33
bination with absent biomechanical stimulation might 34
explain the insufficient bone formation despite adequate 35
expression of bone-related genes. Optimization of the 36
interplay of osteogenic cells and osteo-inductive factors 37
might eventually generate sufficient amounts of axially 38
vascularized bone grafts for reconstructive surgery. 39

40 Abbreviations 42

HA	Hyaluronic acid/hyaluronan hydrogel	43
BMP	Bone morphogenetic protein	44
CT	Computerized tomography	45
A–V	Arterio–venous	46
PLDLLA	Poly(L-lactide-co-D,L-lactide)	47
PCL	Poly(ε-caprolactone)	48
TCP	β-Tri-calcium phosphate	49

A1 S. N. Rath · G. Prymachuk · O. A. Bleiziffer · A. Arkudas ·
A2 J. P. Beier · R. E. Horch · U. Kneser (✉)
A3 Department of Plastic and Hand Surgery, University of Erlangen
A4 Medical Center, Krankenhausstrasse 12, 91054 Erlangen,
A5 Germany
A6 e-mail: Ulrich.kneser@uk-erlangen.de

A7 S. N. Rath · C. X. F. Lam
A8 Division of Bioengineering, National University of Singapore,
A9 21 Lower Kent Ridge Road, Singapore 119077, Singapore

A10 S. T. B. Ho
A11 Graduate Programme in Bioengineering, Yong Loo Lin School
A12 of Medicine, National University of Singapore, 28 Medical
A13 Drive, Singapore 117456, Singapore

A14 D. W. Hutmacher
A15 Faculty of Engineering, Faculty of Science, Institute of Health
A16 and Biomedical Innovation, Queensland University of
A17 Technology, Brisbane, QLD 4000, Australia

52 1 Introduction 52

Bone tissue engineering is based on the application of 53
mechanically stable osteo-conductive scaffolds, osteogenic 54
cells, and osteo-inductive growth factors [1]. Although 55
autologous bone grafts represent the gold standard for the 56
treatment of bone defects, a number of approaches 57
employing osteo-conductive biomaterials had been descri- 58
bed recently, in particular when massive bone loss was 59
present. The creation of large constructs with full viability 60
and functional activity still presents a major challenge. 61
Since cells cannot survive at a distance of more than 62

63 200–500 μm from a capillary, it is imperative for tissue-
64 engineered grafts to be well perfused by a rich vascular
65 network [2, 3]. In addition to the survival of cells, vascular-
66 ization is pre-requisite even for their differentiation [4].

67 In the majority of cases, host blood vessels grow into a
68 biomaterial in a random fashion after implantation *in vivo*, a
69 process called extrinsic vascularization. Transfer to the
70 defect site, though possible, is usually associated with
71 destruction of the vascular network. Thereafter, random
72 network formation among graft and host capillaries is
73 essential for the survival of the graft. On the contrary, a graft
74 pre-vascularized with a surgically created A–V loop forms an
75 axially vascularized tissue [5]. This type of vascularization is
76 desired by reconstructive surgeons because, similarly as in
77 free flap transfer, it can be transferred to the defect site using
78 microsurgical techniques [6]. After implantation, these tissues
79 are immediately vascularized with complete survival of
80 the graft. An axially vascularized bioartificial bone graft was
81 successfully generated recently by our group using an A–V
82 loop as a vascular carrier [5]. The same technology might be
83 further extended for a large bone graft in a sheep model [7],
84 with the addition of suitable osteo-inductive factors.

85 Bone induction is a complex process involving chemo-
86 taxis, mitosis, and differentiation orchestrated by a number
87 of cytokines and growth factors in a sequential manner
88 starting from wound healing to bone remodeling [8].
89 A typical bone induction process takes almost 28 days after
90 bone loss, with the mesenchymal stem cell (MSC) attachment
91 on day three, while vascular invasion starting on day
92 nine [9]. The chemotactic factors induce migration of
93 osteo-progenitor cells to the local site followed by induction
94 of differentiation towards bone lineage and secretion
95 of bone matrix proteins by bone-inducing growth factors,
96 especially BMP-2. Additional BMP group of proteins and
97 VEGF govern cell proliferation and bone vascularization to
98 make viable osseous tissue [8].

99 Bone morphogenetic proteins (BMP-2 s) are part of the
100 TGF- β group of highly active osteoinducing proteins and
101 they played a key role in the creation of many tissue
102 engineered bone grafts in the past [10, 11]. Considering its
103 highly potent action, a controlled release *in vivo* is
104 imperative and deviation of the release in any side can
105 either result in insufficient bone formation or lead to
106 undesired ectopic bone formation, compromising the
107 vitality of nearby tissues [11, 12]. Within 14 days of local
108 BMP-2 application, its concentration decreases to 5% of
109 initial dosage [13]. When BMP-2 is applied as a solution
110 *in vivo*, it is released into the blood stream and loses its
111 bioactivity within hours after rapid degradation and may
112 not be effective for bone induction [14].

113 One major goal for drug delivery systems is to maintain
114 BMP-2 at the site of bone loss and release it in a controlled
115 and continuous manner to act on migrating osteogenic cells

116 to induce bone formation [13]. The release has to be
117 predictable and at physiological concentrations; the BMP-
118 responsive cells should be located nearby. Failure of clinical
119 trials has been reported when its bioavailability was
120 lower than the physiological requirement of the bone
121 healing process because of its rapid degradation after
122 release [15]. To circumvent the problem, increased amounts
123 of BMP-2 at supra-physiologic doses may be given. In
124 addition to increased cost, this may induce ossification
125 impinging on nearby vital neurovascular structures and life-
126 threatening swelling and disability [16]. Though type I
127 collagen is most commonly used for BMP-2 as a carrier
128 [11], a number of other carrier systems have been suggested
129 [13]. In some cases, carrier systems such as fibrin glue are
130 used to inhibit BMP-2 diffusion out of the applied site to
131 prevent soft tissue ossification [12]. Additionally, a carrier
132 acts more than just delivering BMP-2 with documented
133 supra-additive effect of a carrier and BMP-2 forming a
134 favorable three-dimensional extracellular matrix.

135 Hyaluronan (HA) hydrogel is osteo-conductive and
136 osteo-integrative. However, for its osteo-inductive action,
137 special growth factors need to be applied. Currently, BMP-2
138 and BMP-7 have been approved with type I collagen carrier,
139 but other carriers may be superior in terms of efficacy [17].
140 Hyaluronan has been shown to protect growth factors *in*
141 vitro for more than 4 weeks from proteolysis [18]. It has
142 also been shown to release active growth factors slowly in
143 the presence of heparin [18]. Heparin can prolong the stability
144 of BMP-2 almost 20-fold and can produce ectopic
145 bone with only 1 μg of BMP-2, avoiding the use of significantly
146 increased doses [19]. However, for the effective
147 action of BMP-2, angiogenesis and vascular invasion must
148 precede before ossification [9]. Exploiting the ability of
149 BMP-2 to induce ectopic bone, heparin-incorporated hyal-
150 uronic acid hydrogel can be utilized for its delivery.

151 In this experiment, we hypothesize that an axially vas-
152 cularized ectopic tissue-engineered bone graft can be
153 fabricated with an A–V loop surrounding the PLDLLA–
154 TCP–PCL–Hyaluronan scaffold-hydrogel composite. The
155 aim of this study was twofold: firstly, to evaluate the BMP-
156 2 release capacity of the system and growth and survival of
157 primary osteoblasts *in vitro*; secondly, to investigate progress
158 of vascularization and formation of bone tissue
159 within the composites *in vivo* following application of
160 different concentrations of BMP-2 or primary osteoblasts.

161 2 Materials and methods

162 2.1 Scaffold fabrication

163 The scaffolds were fabricated using the fused deposition
164 modeling (FDM) principle [20] utilizing three different

165 materials: PLDLLA (Boehringer-Ingelheim, Ingelheim am
166 Rein, Germany), PCL (Absorbable Polymers, US), TCP
167 (Progentix, MB Bilthoven, Netherlands), in a ratio of 64,
168 16, and 20% by weight, respectively. The strength is pro-
169 vided by the bioceramic component, while the polymer
170 part enables plasticity and ease of fabrication. The fabri-
171 cation was by an in-house rapid prototyping (RP) system,
172 namely the screw extrusion system (SES), similar to FDM
173 [20]. The details of the fabrication method are described
174 elsewhere [21]. Briefly, it exploits a layer-by-layer fabri-
175 cation technique to assemble three-dimensional (3D)
176 structures by depositing two-dimensional (2D) supporting
177 struts based on specified lay-down patterns to assemble the
178 whole structure. Material is fed into the top of the barrel
179 chamber, heated to a molten liquefied state at 120°C and
180 transported towards a 400 µm nozzle with aided displace-
181 ment and pressure from the turning screw feed.

182 Scaffold sheets of 50 × 50 × 1.5 mm³ were fabricated
183 with a 0–90° lay-down pattern. Discs with 8 mm diameter
184 were punched out from it and fabricated into bobbin-shaped
185 constructs (Fig. 1). The scaffolds were uniformly treated
186 with 5 M sodium hydroxide for 5 min and rinsed with
187 de-ionized water to yield a hydrophilic and corrugated sur-
188 face for improved cell attachment [22]. They were sterilized
189 in 70% ethanol overnight followed by UV light for 2 h. The
190 biomechanical properties of a comparable composite scaffold
191 were found to be suitable for bone tissue engineering,
192 showing excellent compatibility with MSCs [21].

193 2.2 Osteoblast culture and analysis in hyaluronan- 194 based hydrogel

195 Primary osteoblasts were isolated from long bones of male
196 Lewis rats as described elsewhere [23]. In brief, after sac-
197 rificing the rats at 4–8 weeks age, the long bones were col-
198 lected and serially digested in sterile collagenase-II (554
199 U/ml, Biochrom AG, Berlin, Germany) in 1 × PBS. Subse-
200 quently, the cells were cultured in flasks (COSTAR, Cam-
201 bridge, USA), maintained at 37°C and 5% CO₂ with twice
202 weekly media change. Only second passage cells were
203 seeded into the scaffold for in vitro and in vivo evaluation.

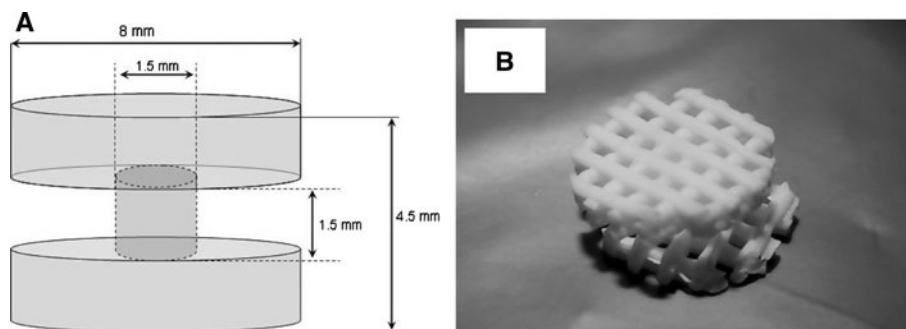
204 The hyaluronan-based (HA) hydrogel (Extracel-HP, 204
205 Glycosan BioSystems, Salt Lake City, Utah) was supplied as
206 a kit consisting of three components, namely thiol-modified
207 hyaluronan and heparin, thiol-modified gelatine, and thiol-
208 modified cross-linker, polyethylene glycol diacrylate. The
209 components were prepared with distilled water at 37°C
210 under aseptic conditions and were mixed at 2:2:1 ratio,
211 respectively, according to the manufacturer's recommen-
212 dations. The osteoblasts were mixed in the hydrogel such
213 that 100 µl of the hydrogel, aliquoted in each well of 96-well
214 culture plate, contained 10,000 osteoblasts. The cells were
215 cultured in a 37°C incubator with 5% CO₂ with 100 µl of
216 media. The medium was changed twice weekly. Osteoblasts
217 in HA were observed for 8 weeks under inverted light
218 microscope (Leica DMIL, Wetzlar, Germany).

219 The hyaluronan-osteoblast specimens were analyzed by
220 AlamarBlue (Biosource Int., Camarillo, CA) assay. Each
221 week, culture medium was aspirated and 150 µl of culture
222 medium with 5% AlamarBlue was added to the specimens
223 and incubated for 4 h at 37°C. Absorbance was then
224 measured with a plate reader (SPECTRAMax 190,
225 Molecular Devices, Sunnyvale, CA, USA) at wavelengths
226 of 570 and 600 nm. The percentage of AlamarBlue
227 reduction was subsequently calculated as advised by the
228 manufacturer.

229 Cell proliferation was evaluated using PicoGreen DNA
230 quantification assay (Molecular Probes, Invitrogen GmbH,
231 Karlsruhe, Germany) at 4 and 8 weeks as advised by the
232 manufacturer. Specimens were thoroughly destroyed with
233 lysis buffer (10 mM Tris (pH 7.0), 1 mM EDTA, and
234 0.2% v/v triton X-100; all from Sigma-Aldrich GmbH,
235 Steinheim, Germany). Fluorescence of specimen wells was
236 measured with a fluorescent microplate reader (Genios,
237 Tecan Group Ltd, Maennedorf, Switzerland) at excitation
238 and emission wavelengths of 485 and 535 nm, respec-
239 tively, corrected with blanks.

240 To visualize viable and non-viable cells, osteoblasts
241 were labeled with fluorescent probes. The osteoblast-
242 seeded hydrogels were washed with 1 × PBS and incubated
243 with 2 µg/ml fluorescein diacetate (FDA) (Molecular
244 Probes Inc., Eugene, USA) in 1 × PBS, for 15 min at 37°C.

Fig. 1 a Schematic diagram of the bobbin-shaped scaffold.
b The scaffold showing high porosity and a central groove for accommodating the A–V loop



245 They were gently rinsed twice in $1 \times$ PBS and placed in
 246 $20 \mu\text{g/ml}$ propidium iodide (PI) solution (Invitrogen
 247 GmbH, Karlsruhe, Germany) for 2 min at room tempera-
 248 ture. After thorough rinsing in $1 \times$ PBS, the specimens
 249 were kept in $1 \times$ PBS and viewed under a fluorescent
 250 microscope (Axiovert 25, Carl-Zeiss AG, Goettingen,
 251 Germany). The viable cell cytoplasm was labeled green,
 252 while non-viable cell nuclei were labeled red.

253 2.3 Release kinetics of rhBMP-2 from hyaluronan- 254 based hydrogel

255 The rhBMP-2 (INFUSE bone graft, Medtronic, Minne-
 256 apolis, USA) was reconstituted to final concentration of
 257 $3.33 \mu\text{g}/\mu\text{l}$ in PBS. $10 \mu\text{g}$ of rhBMP-2 was incorporated in
 258 $50 \mu\text{l}$ of hyaluronan hydrogel. All disc shaped hydrogels
 259 were uniformly polymerized to get a thickness of 4 mm
 260 and a diameter of 5 mm. The BMP-2 containing hydrogel
 261 discs ($n = 3$) were placed in 1 ml of pre-warmed PBS until
 262 35 days from the start of the experiment. At different time
 263 points (1, 2, 4, 6, and 24 h and 2, 4, 7, 10, 14, 17, 21, 28,
 264 and 35 days), $100 \mu\text{l}$ of PBS were sampled and replaced
 265 with an equal amount of fresh PBS after the scaffolds were
 266 kept on a shaker for 3 min. The collected $100 \mu\text{l}$ of PBS
 267 were kept in -80°C and the rhBMP-2 content was mea-
 268 sured by rhBMP-2 ELISA kit (Quantikine, R&D systems,
 269 Minneapolis, MN, USA). The values were calculated from
 270 the standard curve. The cumulative release was calculated
 271 for each time point.

272 2.4 In vivo experiments

273 Twenty-four inbred male Lewis rats (Charles-River, Sulz-
 274 feld, Germany) weighing 200–300 g were used with
 275 approval by the animal care committee of the University of
 276 Erlangen and the Government of Mittelfranken, Germany.
 277 Animals were kept in 12 h dark–light cycle with free
 278 access to standard chow (Altromin, Hamburg, Germany)
 279 and water at the veterinary care facility of the University of
 280 Erlangen Medical Center. All operations were performed
 281 by experienced microsurgeons using a surgical microscope
 282 (Karl Zeiss, Jena, Germany) under general anaesthesia with
 283 Isoflurane (Baxter, Unterschleißheim, Germany).

284 The rats were divided into four groups, each consisting
 285 of six animals. The PLDLLA–TCP–PCL scaffold was
 286 loaded with 1 ml of HA hydrogel containing either of
 287 500 ng rhBMP-2 (group A), $2.5 \mu\text{g}$ rhBMP-2 (group B), or
 288 three million hydrogel-immobilized osteoblasts (group C)
 289 prior to implantation. Scaffolds with plain HA hydrogel
 290 served as controls (group D).

291 The surgical technique has been described previously by
 292 our group [24]. In brief, the femoral vessels and nerve were
 293 exposed by a longitudinal incision from the inguinal

ligament to the knee. The sheath of the neurovascular
 bundle was opened. After exposure of the right-sided
 femoral vessels, a 20 mm vein graft was harvested from the
 right femoral vein. An A–V loop was created by interpo-
 sition of the vein graft between the left sided femoral artery
 and the left femoral vein with interrupted non-absorbable
 11-0 nylon stitches (Ethilon, Ethicon GmbH, Norderstedt,
 Germany). The A–V loop was placed around the PLD-
 LLA–TCP–PCL scaffold and the whole construct was
 placed into a sterile cylindrical Teflon-chamber (inner
 diameter 10 mm, height 6 mm, constructed by the Institute
 of Materials Research, Division of Glass and Ceramics,
 University of Erlangen). The chamber was then capped
 and fixed to the underlying muscle. The skin was closed
 using interrupted 3-0 vicryl sutures (Ethicon GmbH,
 Norderstedt, Germany). All animals received 0.2 ml ben-
 zylpenicillinbenzathine (Tardomycel; Bayer, Leverkusen,
 Germany), buprenorphine (0.3 mg/kg rat weight) (Tem-
 gesic; Essex Chemie AG, Luzern, Switzerland), and hep-
 arin (80 IU/kg) (Liquemin; Ratiopharm, Ulm, Germany)
 postoperatively.

Explantation of the specimens was performed after
 8 weeks. For sacrifice, one specimen from each group was
 used for RNA isolation as described later. The other rats
 were perfused with Microfil under general anesthesia for
 micro-CT analysis. The aorta was cannulated and the
 vascular system was rinsed with heparinized Ringer solu-
 tion (100 IU/ml) under hydrostatic pressure. The distal
 vascular system was then injected with 20 ml microfil
 (MV-122) containing 5% of MV curing agent (both from
 Flowtech, MA, USA) as advised by the manufacturer.
 Finally the aorta and caval vein were ligated and the rats
 were cooled at 4°C for 24 h. Specimens were explanted in
 toto and fixed in 3.5% formalin solution before micro-CT.

298 2.5 Micro-CT analysis

For each of the experimental groups, two specimens were
 selected at random for micro-CT analysis. To decalcify the
 scaffolds, the explanted grafts were treated with 20% EDTA
 for 3 weeks before further manipulation. They were sub-
 sequently scanned on a high resolution ‘‘ForBild’’ scanner
 (an in vivo micro computerized tomography (micro-CT)
 scanner developed by Institute of Medical Physics, FAU
 Erlangen-Nuremberg, Germany). The constructs were
 scanned with following parameters: Al-0.5 mm filter, tube
 voltage of 40 kV, $15 \mu\text{m}$ pixel size, and $15 \mu\text{m}$ slice dis-
 tance between consecutive slices. The data were volumet-
 rically re-constructed using ImpactView software (Vamp
 GmbH, Erlangen, Germany) in a 1024×1024 pixels
 matrix. Further, 3D modeling for data analysis was
 done using Mimics v8.02 software (Materialise, Leuven,
 Belgium). The different tissues were segmented according

345 to their Hounsfield Unit values by global thresholding
346 procedure to selectively obliterate the scaffolds and soft
347 tissues. After 3D reconstruction, the volume and area of
348 microfil-perfused blood vessels were calculated. Using the
349 data, the mean number of vessels per unit length was cal-
350 culated, as described before [25].

351 2.6 Histology and histomorphometry

352 The samples were serially dehydrated and paraffin
353 embedded according to standard protocols. Five μm sec-
354 tions were taken using a microtome (Leica RM 2135,
355 Wetzlar, Germany). All the slides were stained with
356 Hematoxylin and eosin (H & E) using a fully automated
357 process (Jung Auto Stainer XL, Leica Microsystems,
358 Nussloch, Germany).

359 Immunohistochemical analysis was performed using
360 rabbit polyclonal antibodies against vWF (von-willebrand
361 factor) (A0082, Dakocytomation, Carpinteria, CA, USA)
362 at 1:500 dilution to confirm the vascular endothelium.
363 Envision HRP anti-rabbit kit (K4011, Dakocytomation,
364 Carpinteria, CA, USA) was used as secondary antibody.

365 The histomorphometric analysis was performed by two
366 blinded, independent observers as described elsewhere
367 [26]. Briefly, the images of two standardized planes
368 (500 μm proximal and 500 μm distal to the central plane)
369 were photographed and oriented perpendicular to the lon-
370 gitudinal axis of A–V loops. All images were taken by a
371 light microscope with bright-field filter (Leica DM IRB,
372 Wetzlar, Germany) and digital camera under $\times 25$ magni-
373 fication. The individual images of each cross section were
374 set together (Photoshop, Adobe, San Jose, CA, USA). The
375 composed images were rendered bimodal (ImageJ, NIH,
376 Bethesda, MA, USA). The construct size (cross-sectional
377 area) and the area of FVT were measured for each of the
378 sections. The percentage of fibro vascular tissue (% FVT)
379 was calculated by the ratio of total FVT area to total cross
380 sectional area of the specimen. The total number of blood
381 vessels was assessed by counting the microfil-filled (posi-
382 tive) vessels in ten pre-selected fields of view (four in the
383 central region and three each in upper and lower parts of
384 the construct) at $\times 100$ magnification. Results are expressed
385 as means \pm standard-errors of the mean.

386 2.7 RNA isolation and quantitative real time RT-PCR

387 After scarification of the animal, the chamber was quickly
388 isolated and kept overnight at 4°C in RNAlater RNA
389 Stabilization Reagent (Qiagen, Hilden, Germany) and fur-
390 ther in -80°C until RNA isolation. Total RNA was isolated
391 from the tissue grown in the loop using TRIzol Reagent
392 (Invitrogen, Carlsbad, CA, USA) followed by RNeasy Mini
393 Kit (Qiagen, Hilden, Germany) according to manufacturer's

394 protocol and RNA was measured by BioPhotometer 394
(Eppendorf, Hamburg, Germany). Total RNA was con- 395
verted to c-DNA using oligo d-T primers (Fermentas, Glen 396
Burnie, MD, USA) and RevertAid H Minus M-MuLV 397
Reverse Transcriptase (Fermentas, Glen Burnie, MD, USA). 398

399 The amount of cDNA corresponding to 20 ng of total 399
RNA was then analyzed in triplicates by semi-quantitative 400
real time PCR for selected genes with primers as shown in 401
Table 1 by Mx3000P QPCR System (Stratagene, Agilent 402
technologies, La Jolla, CA, USA). The gene expressions 403
were normalized to internal β -actin expression and the 404
relative fold change was expressed by comparing to that of 405
control group D. 406

407 2.8 Statistical analysis

408 Statistical comparisons were performed for histomorpho- 408
metric analysis by a two-way ANOVA test followed by 409
Bonferroni's post-test (Sigmastat v3.5, Chicago, IL) con- 410
sidering significant difference at the 95% confidence 411
interval. Standard error bars were included in all graphs 412
and represent the 95% confidence interval. For all pairwise 413
comparisons on quantitative results the Student's *t*-test was 414
used with a confidence level of 95% ($P < 0.05$). 415

416 3 Results

417 3.1 Osteoblasts in hyaluronan-based hydrogel in vitro

418 At 4 and 8 weeks, osteoblasts were relatively distinct and 418
well maintained throughout the hydrogel (Fig. 2a). How- 419
ever, the thickness of the hydrogel decreased considerably 420
over 8 weeks. Vitality of osteoblasts was demonstrated 421
over the entire observation period by FDA/PI staining 422
(Fig. 2b) while dead cells were almost non-existent. 423

424 The metabolic activity of the cells increased progres- 424
sively until week five followed by a decline by week eight 425
(Fig. 2c). A similar trend was observed in the DNA 426
quantification assay, where a significant decrease in 427
dsDNA values between week four (35.38 ± 10.34) and 428
week eight (7.57 ± 1.90) was demonstrated (Fig. 2d). 429

430 3.2 Release kinetics of BMP-2 from hyaluronan-based 430 hydrogel 431

432 In vitro BMP-2 release from HA hydrogels was followed 432
until day 35 (Fig. 3). The release kinetics of BMP-2 was 433
characterized by a fast initial peak within the first 3 days 434
followed by a sustained release over the course of 35 days. 435
Even at the end of 5 weeks, a considerable percentage of 436
BMP-2 was still incorporated inside hydrogel. Within the 437
first 24 h, almost 10% of the loaded BMP-2 was released. 438

Table 1 The primers of the genes analyzed by real time PCR

Gene name	Forward primer	Reverse primer
Alkaline phosphatase	GCTGATCACTCCCACGTTTT	GCTGTGAAGGGCTTCTTGTC
Biglycan	CCACCAACTAACCAGCCTGT	CAAGGTGAAGTCCCAGAAGC
Syndecan	CTGATCCTGCTGCTGGTGTA	TCATGCGTAGAACTCGTTGG
BMP 2	TGAACACAGCTGGTCTCAGG	TTAAGACGCTTCCGCTGTTT
Osteocalcin	CTATGGCACCACCGTTTAGG	AGCTGTGCCGTCCATACTTT
Collagen 1	TTCTGAAACCCTCCCCTCTT	CCACCCCAGGGATAAAAACT
Osteonectin	AAACATGGCAAGGTGTGTGA	AAGTGGCAGGAAGAGTCGAA
Agrrecan	AACTCAGTGGCCAAACATCC	AGATGTTCCCTCACCAGTGC
Collagen 2	CGAGGTGACAAAGGAGAAGC	AGGGCCAGAAAGTACCCTGAT
VEGF	AATGATGAAGCCCTGGAGTG	ATGCTGCAGGAAGCTCATCT
Beta-actin	GATCATTGCTCCTCCTGAGC	ACATCTGCTGGAAGGTGGAC
FGF 2	TTCTTTGAACGCCTGGAGTC	CCGTTTTGGATCCGAGTTTA

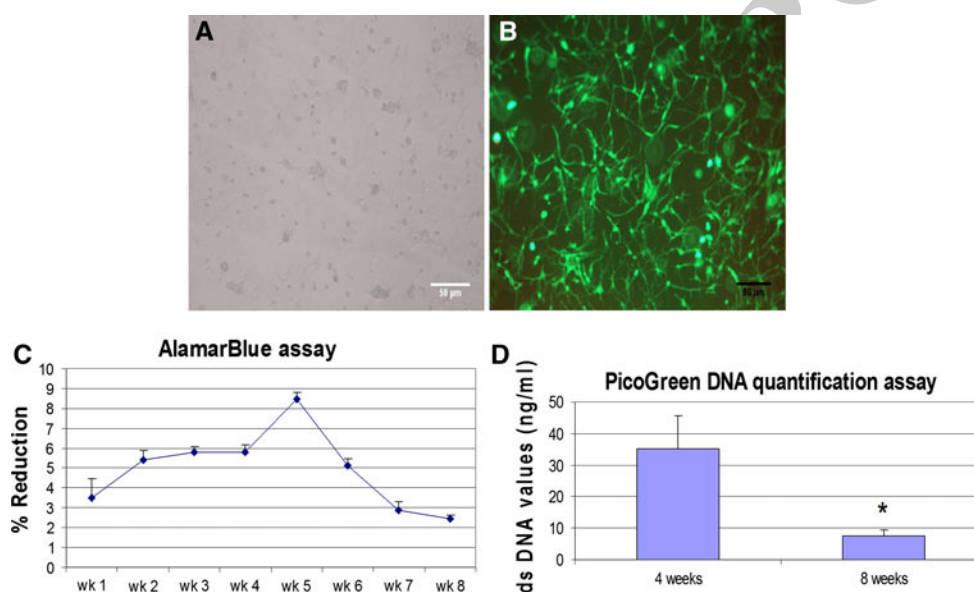


Fig. 2 Osteoblasts in hyaluronic acid hydrogel after 4 weeks, examined in **a** inverted light microscope, and **b** after FDA/PI staining in fluorescence microscope. Cells are evenly distributed within the matrix and display a typical and differentiated morphology. There are virtually no dead (PI-positive) cells. **c** Metabolic activity of osteoblasts

is demonstrated by AlamarBlue assay in hyaluronic acid hydrogel over the observation period with a peak at week five. **d** The dsDNA value of osteoblasts is significantly decreased at week eight compared to week four as evidenced by PicoGreen assay ($P < 0.05$)

439 Thereafter, the release rate was almost constant until the
440 end of observation.

441 3.3 Qualitative and quantitative micro-CT analysis

442 The pattern and distribution of angiogenesis of representa-
443 tive samples in micro-CT scanning are shown for scaffolds
444 with plain hydrogel (control group D, Fig. 4d), hydrogel
445 with low dose BMP-2 (500 ng, group A, Fig. 4a), hydrogel
446 with high dose BMP-2 (2.5 μ g, group B, Fig. 4b), and
447 hydrogels containing osteoblasts (group C, Fig. 4c). In

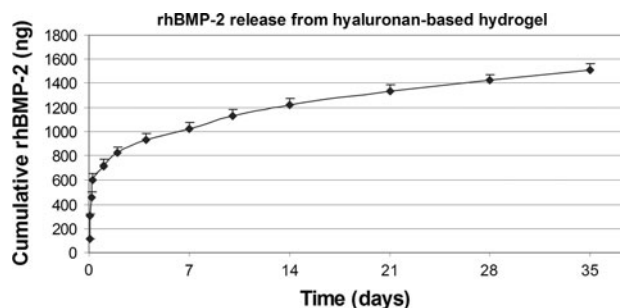
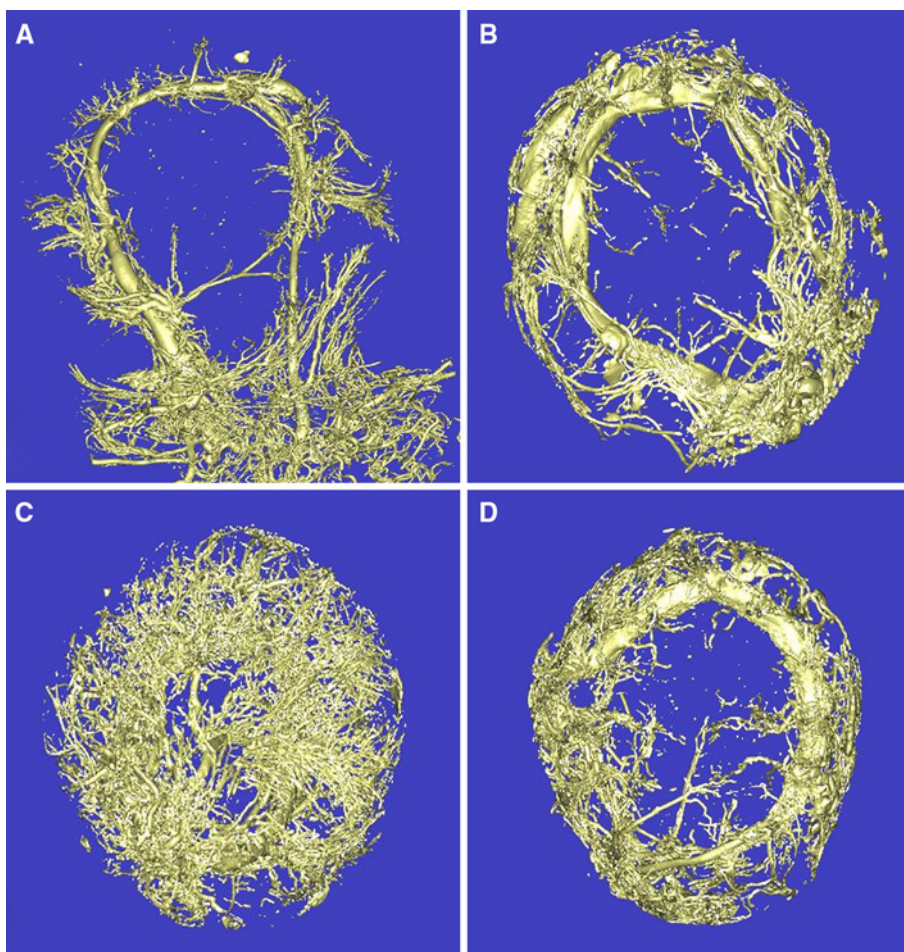


Fig. 3 Cumulative release of rhBMP-2 from the hyaluronic acid hydrogel over a period of 35 days

Fig. 4 Micro-CT analysis. 3D reconstructed images of representative samples from **a** group A (500 ng/ml BMP-2), **b** group B (2.5 µg/ml BMP-2), **c** group C (osteoblast transplanted), and **d** group D (control). Osteoblast transplantation leads to considerable increase in blood vessel outgrowth from the A–V loop



448 groups A and D, blood vessels start sprouting from the A–V
 449 loop into the centre of the scaffold. In group B, the newly
 450 grown vessels already extend towards the centre of the
 451 scaffold from all directions. However, only in group C
 452 (osteoblast transplantation) there is extensive vascular
 453 growth filling the entire centre of the scaffold (Fig. 4d).

454 The total volume of angiogenesis approached 5–10 mm³
 455 in control group D as well as groups A and B (low dose
 456 BMP-2 and high dose BMP-2, respectively) (Fig. 5a).
 457 However, in group C (osteoblast transplantation) the value
 458 was 10–15 mm³. As per the calculation by Bolland et al.
 459 [25], the number of vessels per mm length in groups A, B,
 460 and D is within 10–100, while one group C sample shows
 461 187 per mm length (Fig. 5b). No further statistical analysis
 462 of the micro-CT data was performed due to the limited
 463 number of samples (Fig. 5b).

464 3.4 Histology and immunohistochemistry

465 Histological specimens showed numerous microfil-filled
 466 blood vessels (black) in specimens from all groups.
 467 A dense network of newly formed blood vessels originated
 468 from the A–V loop and progressively invaded the void

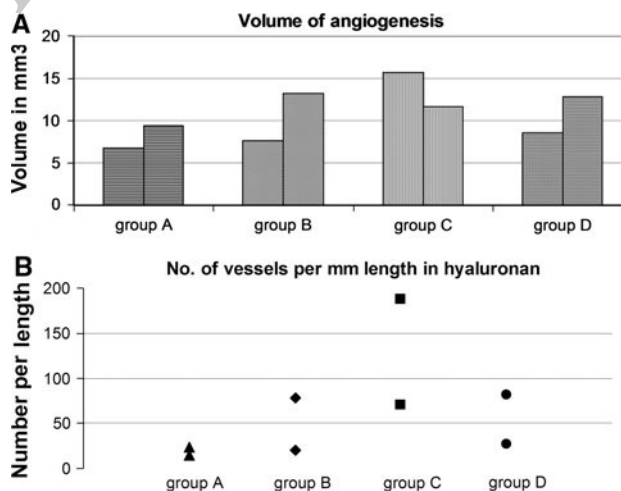


Fig. 5 Quantitative micro-CT analysis of specimens after 8 weeks in vivo (*n* = 2 per group) showing **a** the volume of angiogenesis in the isolation chamber, and **b** number of vessels per mm length

spaces within the scaffolds from all groups. However, 469
 BMP-2 concentration and transplantation of osteoblasts 470
 influenced the number of blood vessels and the volume of 471
 newly formed fibro-vascular tissue. A representative figure 472

Author Proof

473 of each type of sample is shown in Fig. 6: low concentration of BMP-2 (group A, Fig. 6a), high concentration of BMP-2 (group B, Fig. 6b), osteoblast transplantation (group C, Fig. 6c), and scaffolds with plain hydrogel (control group D, Fig. 6d). There was no significant foreign body reaction detectable in specimens from any group and the scaffolds were almost completely intact after 8 weeks. In specimens from groups A, B, and D (low concentration BMP, high concentration BMP and control, respectively), there was some amount of non-resorbed hyaluronan matrix observed after 8 weeks. In contrast, in specimens from group C (osteoblast transplantation), the hydrogel component was completely resorbed.

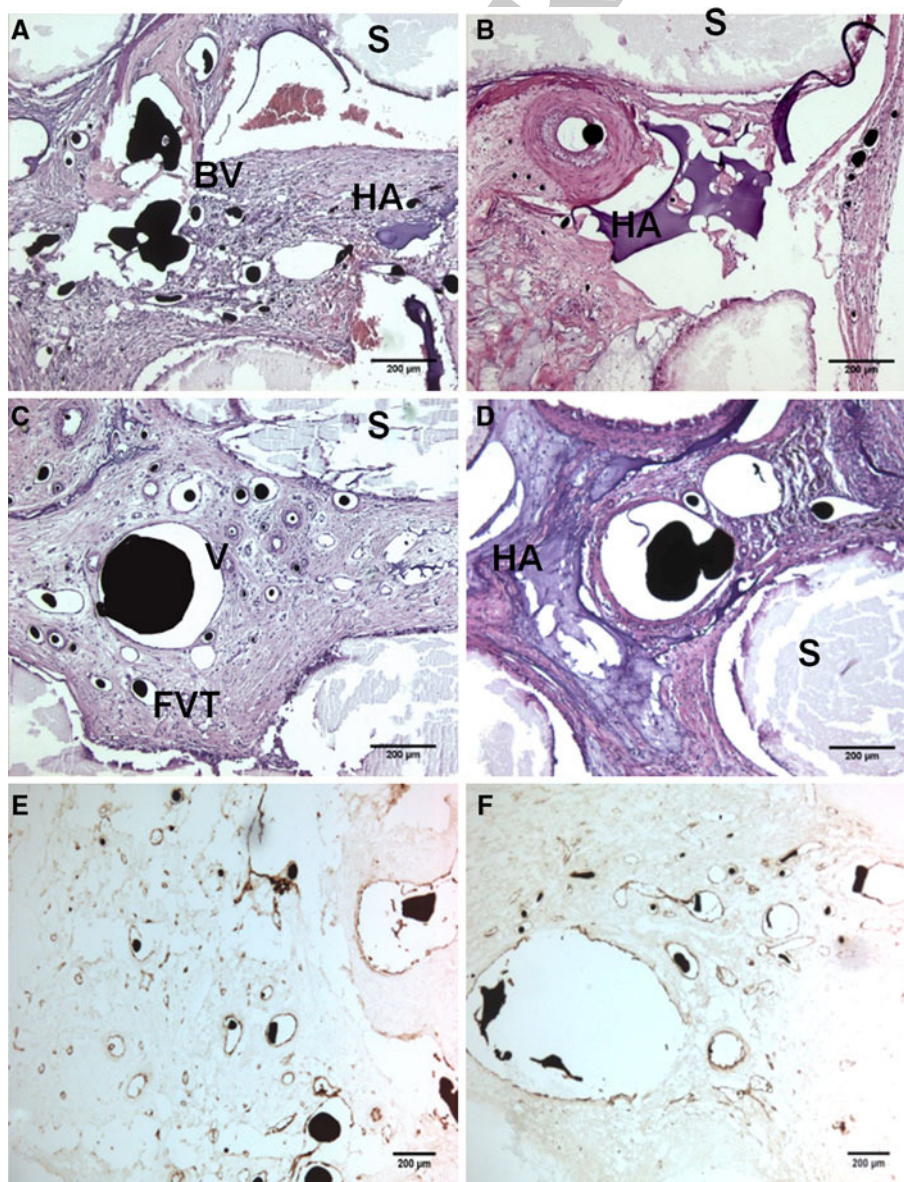
486 Immunostaining with vWF antibody specifically demonstrated patency and functional integrity of blood vessels

488 with microfil-filled (black) lumen in specimens from all groups (Fig. 6e, f). There was no significant bone formation detectable in histological samples from any group.

3.5 Histomorphometry

492 The percentages of fibro vascular tissue (FVT) were for group A 12.57 ± 1.3 , for group B 16.52 ± 0.7 , for group C 24.14 ± 1.4 , and for group D 16.28 ± 2.6 , respectively. Similarly, the percentages of unresorbed hyaluronic acid matrix left at the end of 8 weeks were 15.34 ± 3.1 , 5.76 ± 1.0 , 0 ± 0 , and 13.62 ± 2.1 for groups A, B, C, and D, respectively. Interestingly, the entire hyaluronic acid hydrogel was resolved in group C (osteoblast transplantation) specimens. The percentage of FVT was

Fig. 6 Hematoxylin and eosin staining of representative specimens: **a** group A (500 ng/ml BMP-2), **b** group B (2.5 μ g/ml BMP-2), **c** group C (osteoblast), and **d** control group D after 8 weeks. *S* scaffold, *HA* hyaluronic acid matrix, *BV* microfil-filled blood vessels, *FVT* fibro vascular tissue, *V* vein of the loop. All scale bars show 200 μ m. (**e** and **f**) Immunohistochemistry with vWF antibody showing the vascular architecture of group B and group D, respectively. The co-localization of vWF-positive walls and microfil-filled lumen clearly demonstrate functional integrity of the newly grown vasculature



501 significantly higher ($P < 0.001$) in samples from group C
 502 in comparison to groups A, B, and D. The percentage of
 503 hyaluronic acid hydrogel matrix values was significantly
 504 lower in groups B and C compared to groups A and D.
 505 The results are displayed graphically in Fig. 7a.

506 The total number of blood vessels per cross section area
 507 was 95.57 ± 23.40 , 66.40 ± 3.91 , 138.7 ± 9.60 , and
 508 67.33 ± 12.03 in groups A, B, C, and D, respectively.
 509 Specimens from the osteoblast transplantation group C
 510 contained significantly more blood vessels than specimens
 511 from groups B and D ($P = <0.05$) (Fig. 7b).

512 3.6 Quantitative real time RT-PCR

513 Bone-related gene expression profile is shown in Fig. 8.
 514 Expression of collagen-I and osteonectin was not significantly
 515 increased in the experimental groups A–C in
 516 comparison to control group D. In contrast, alkaline
 517 phosphatase, RUNX-2, osteocalcin, and IBSP expressions
 518 were increased in groups A, B, and C (low-and high con-
 519 centration BMP and osteoblast transplantation). However,
 520 this effect was not statistically significant for all groups.

521 Expression profile for selected extracellular matrix
 522 proteins and growth factors are shown in Fig. 9. Syndecan
 523 expression was neither influenced by BMP-2 nor trans-
 524 plantation of osteoblasts. Interestingly, biglycan expression
 525 was increased in high-concentration BMP-2 and osteoblast
 526 transplantation groups (groups B and C, $P < 0.05$ only for
 527 group B). The expression profile of growth factors such as
 528 VEGF, FGF2, and BMP-2 was not significantly different in
 529 the experimental groups A–C compared to control group D.

4 Discussion

531 This study clearly demonstrates that the hyaluronan-based
 532 matrix supported growth and differentiation of osteoblasts
 533 in vitro and in vivo and allowed sustained release of BMP-
 534 2. The whole system showed positive evidence of bone-
 535 related gene expression, though it eventually failed to
 536 induce significant amounts of bone histologically in an
 537 isolation chamber model of axial vascularization. Sum-
 538 marizing, PLDLLA–TCP–PCL polymer-ceramic compos-
 539 ite scaffolds combined with HA-based hydrogel might be
 540 utilized in engineering of bio-artificial bone tissues.

541 Typical hydrogel systems are characterized by an initial
 542 higher peak of growth factor release followed by a reduced
 543 release later. At the beginning, there is maximal avail-
 544 ability of free growth factors for nearby cells [27, 28].
 545 Afterwards, two distinctive release patterns are seen for
 546 different hydrogels. In surface-eroding hydrogel, there
 547 follows a slow release later in time; while in bulk-eroding
 548 hydrogel, degradation and random release ensue [29].
 549 Though the hydrogel is required to bind BMP-2, the con-
 550 tinuous release must induce sufficient concentration in the
 551 vicinity to act on precursor cells to induce the specific
 552 action of the growth factor. In our study, a similar trend
 553 regarding the amount and rate of release of BMP-2 is seen
 554 at the beginning, followed by a very slow release rate until
 555 5 weeks. The final disintegration might have released all
 556 BMP-2 contained in the hydrogel.

557 The hyaluronan hydrogel demonstrated in vitro growth
 558 compatibility with the osteoblasts and supported their rep-
 559 lication, as observed in light microscopic pictures and
 560 corroborated by AlamarBlue results until week five.
 561 Thereafter, the progressive decline in AlamarBlue assay
 562 might be due to gradual dissolution of hydrogel by hyal-
 563 uronidase secreted by osteoblasts with corresponding loss
 564 of cells [30]. This was substantiated by PicoGreen assay,
 565 where 8 week dsDNA was significantly lower than
 566 4 weeks. Cell death cannot account for the lowered values
 567 as all cells were found healthy and alive in FDA/PI staining.

568 Successful vascularization of composite scaffolds was
 569 clearly demonstrated by micro-CT and histological analy-
 570 sis. In micro-CT angiograms, there was significant angio-
 571 genetic activity originating from the original A–V loop. In
 572 BMP groups (groups A and B), the proximal part of loops
 573 generally displayed comparatively more sprouting blood
 574 vessels than the distal part found interior in the chamber.
 575 This might be due to VEGF mediated vascularization by
 576 BMP-2 [31]. In osteoblast transplanted group C, there were
 577 a uniform extensive angiogenetic activity and formation of
 578 blood vessels throughout the chamber, even extending to
 579 the centers. The data were corroborated well by histo-
 580 morphometric analysis. The FVT area as well as the
 581 number of blood vessels was significantly increased in

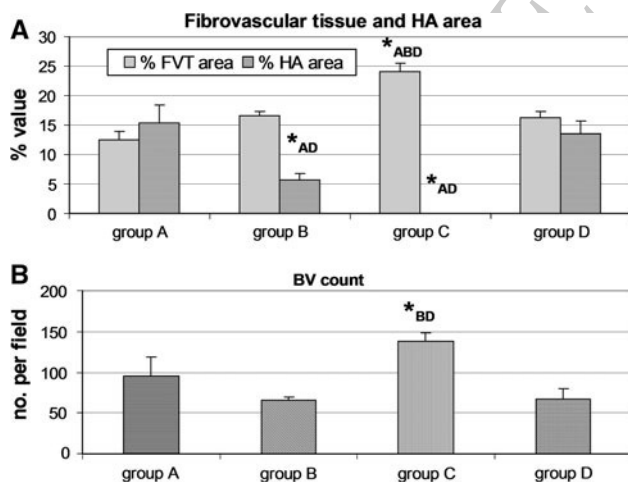


Fig. 7 Histomorphometric calculations of blood vessel formation in the graft constructs. **a** Mean percentage of FVT and non-resorbed hyaluronic acid matrix. **b** Mean number of blood vessels per cross section. Asterisks indicate statistically significant differences between groups ($P < 0.05$); group A 500 ng/ml BMP-2, group B 2.5 μ g/ml BMP-2, group C osteoblast transplantation, and group D control

Fig. 8 Quantitative real time RT-PCR analysis of bone-related gene expression: Collagen-I (a), alkaline phosphatase (b), IBSP (c), RUNX-2 (d), osteocalcin (e), and osteonectin (f). Specific gene expression was normalized to internal β -actin expression. Values represent the fold change compared to control group D. The error bar represents standard deviation and the asterisks indicate significant differences between experimental groups and control group D ($P = 0.05$). Each bar represents three independent measurements. Group A 500 ng/ml BMP-2, group B 2.5 μ g/ml BMP-2, group C osteoblast transplantation, and group D control

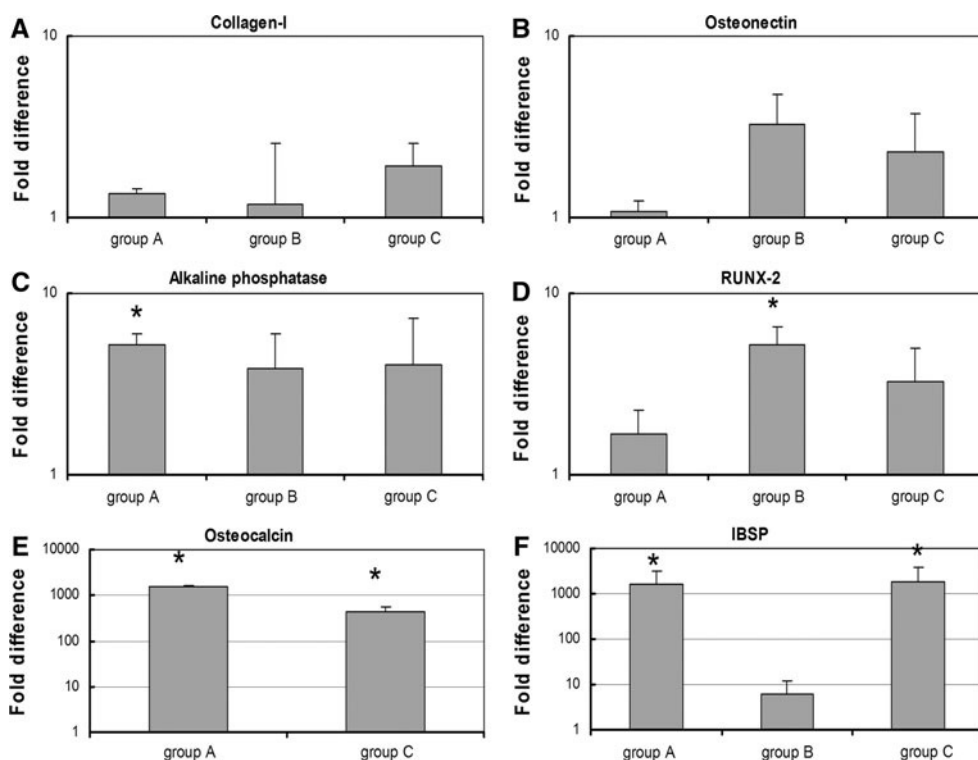
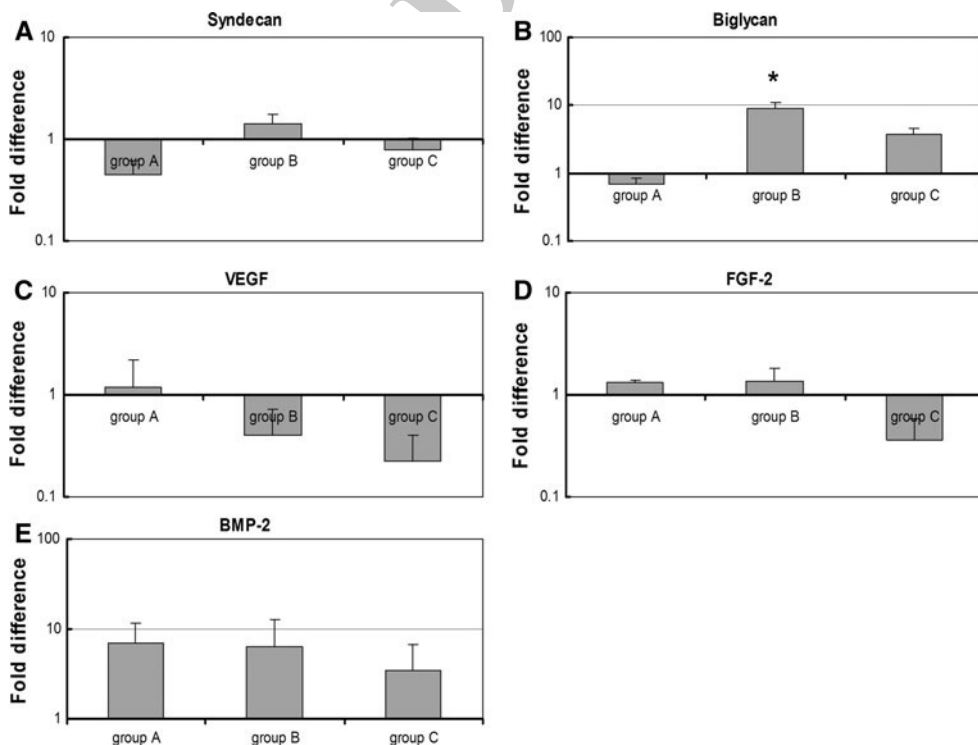


Fig. 9 Quantitative real time RT-PCR analysis of extracellular matrix and growth factors expressions: Syndecan (a), Biglycan (b), VEGF (c), FGF-2 (d), and BMP-2 (e). Specific gene expression was normalized to internal β -actin expression. Values represent the fold change compared to control group D. The error bar represents standard deviation and the asterisks indicate significant differences between experimental groups and control group D ($P = 0.05$). Each bar represents three independent measurements. Group A 500 ng/ml BMP-2, group B 2.5 μ g/ml BMP-2, group C osteoblast transplantation, and group D control



582 group C specimens. These findings might be explained by
 583 faster resorption of hyaluronic acid following application
 584 of osteoblasts [30]. This is supported by significantly lower
 585 percentage of remaining hyaluronan matrix in group C
 586 specimens (Fig. 7). The degradation byproducts may
 587 stimulate angiogenesis subsequently [32]. Additionally, a

strong hypoxic stimulus from cells may stimulate VEGF secretion [33].

Contrary to the demonstration of extensive vascularization, a clear histological evidence of bone formation could not be seen in the examined sections of our loop model. Researchers have tried BMP-2 dosage from 1 μ g in

588
 589
 590
 591
 592
 593

594 hind-limb muscle and subcutaneous tissue to 50 μg in bone
595 defect sites in rats with successful bone induction [34, 35].
596 We have also demonstrated extensive bone formation his-
597 tologically after subcutaneous application of 2.5 μg of
598 BMP-2 after 8 weeks (data not shown). The absence of
599 bone histology in experimental specimens might be due to
600 ineffective dosage of BMP-2, which could only be
601 addressed empirically. The currently approved effective
602 dose with a collagen carrier requires BMP-2 in milligram
603 amounts, while in vivo the level is actually in nano to pico
604 molar range [17]. The higher BMP-2 dose might be nec-
605 essary for ectopic osteoinduction, where there is no readily
606 available effector tissue present.

607 Another reason might be the challenging properties of
608 the isolation chamber model. Since the newly grown tissue
609 was isolated from surrounding tissues except for the
610 communication through vascular loops, the model had
611 limited access to subcutaneous tissue. Previous studies in
612 our model demonstrated that the neo-angiogenesis and the
613 subsequent FVT invasion occur only after 2–4 weeks of
614 surgical loop placement [24]. Beforehand, there might be
615 no effector cells in the adjacent area. By this time, a large
616 percentage of BMP-2 must have been released and biode-
617 graded without any action. With its slow release phase after
618 2 weeks, the local concentration must be grossly inade-
619 quate in inducing ectopic bone. Observations by others
620 support this hypothesis, when they found that application
621 of BMP-2 at a delayed interval of 7 days after the time of
622 surgery resulted in a significantly increased osteogenic
623 induction [28] due to the increased number of BMP-2
624 responsive cells. However, in a separate study, fast release
625 of BMP was associated with increased new bone induction
626 over a short observation period, while a slow release was
627 not [27]. Consequently, it appears that it is the release
628 kinetics of BMP-2 with its net balance of effective con-
629 centration and degradation, which usually makes the dif-
630 ference. The release kinetic must be optimized for our
631 chamber model, where a peak release is required at the
632 time of rapid angiogenesis and FVT generation. Therefore,
633 specifically for this A–V loop model, we may need a higher
634 dosage of BMP-2 or later application during the course of
635 the experiment. In the future, we propose a 2 week delay
636 for BMP-2 application, where the burst release can be
637 synchronized with presumptive maximum vascular tissue
638 growth. Additionally, without proper mechanical stimula-
639 tion, it is unlikely to find significant amounts of mature
640 bone histologically or the induced bone might have even
641 resorbed [36].

642 In comparison to growth factors, co-culture systems are
643 attractive in addressing two components of a tissue such as
644 the osteogenic compartment and blood vessels in bone
645 tissue. Optimally, different cell components are capable of
646 inducing each other to a fully differentiated state. However,

647 regarding applications in regenerative medicine, autolo-
648 gous cells are the gold standard at the moment. Isolation
649 and expansion of autologous cells under GMP conditions,
650 which are mandatory for clinical application of bioartificial
651 tissues, are technically demanding and rather expensive.
652 Additionally, the bi-directional interaction of cells under
653 co-culture conditions needs to be fully characterized. Large
654 volume applications of bioartificial tissues are also ham-
655 pered by significant initial cell loss if vascularization
656 aspects are not considered. Growth factors such as BMPs
657 might be utilized to enhance tissue formation and increase
658 efficacy of cell based strategies [6]. Under certain condi-
659 tions and in selected indications, they might even replace
660 transplantation of cells if adequate release kinetics and
661 material properties are provided.

662 Though the histological cut sections showed no bone
663 formation, semi-quantitative real time PCR results showed
664 a different picture of gene expression. Groups A (500 ng
665 BMP-2) and C (osteoblasts) had significantly higher
666 expression of bone-related genes especially, osteocalcin
667 and IBSP. Group A also showed significantly increased
668 expression of alkaline phosphatase. Expression of these
669 bone-related genes is important at different stages of bone
670 maturation. As histological bone formation is a very
671 complex phenomenon, which requires coordinated inter-
672 play of different types of cells and growth factors, we
673 assume that the osteo-inductive stimulus was sufficient to
674 induce expression of bone-related genes but induction of
675 bone formation eventually failed due to insufficient long-
676 term concentration of BMPs and lack of effector cells. The
677 expression of growth factors such as BMP-2, FGF-2, and
678 VEGF were not significantly different at 8 weeks. Cell
679 surface proteoglycans function in cell adhesion to cell or
680 matrix. A higher expression of biglycan was found in group
681 B (2.5 μg BMP-2), while there was no difference of
682 Syndecan expression. Syndecan is ubiquitously expressed
683 in all cells except for some bone-specific subtypes, while
684 biglycan is highly expressed in bone morphogenesis [37].
685 Cell mitosis can occur at pico molar range of BMP-2, while
686 cell differentiation needs nano molar range [9]. When
687 BMP-2 is sequestered in extracellular matrix, local con-
688 centration might be higher to produce sporadic induction.
689 This might explain the positive bone-related gene expres-
690 sion while absence of any clearly demarcated histological
691 bone.

692 Although a well-vascularized scaffold is essential for the
693 survival of osteoblasts, we have surprisingly found that the
694 presence of cells is also crucial for development of
695 extensive axial vascularization in a reciprocal manner.
696 Therefore, the chamber model could be made porous in
697 future by further modification to have access to the sur-
698 rounding area, making both simultaneous extrinsic and
699 axial vascularization possible at a very early stage.

700 The approach may not only induce survival and faster
701 differentiation of osteoblasts but also stimulate in-growth
702 of new blood vessels. Moreover, application of angioge-
703 netic growth factors such as VEGF might have a similarly
704 stimulating effect. As discussed earlier, BMP-2 and oste-
705 oblasts might be applied in pre-vascularized scaffold after
706 2 weeks delay for their most efficient action, which is
707 currently under investigation by our group. Though such an
708 approach makes the model complex, it may ensure the
709 survival of cells and their differentiation from the
710 beginning.

711 At present, each of the individual components of PLD-
712 LLA–TCP–PCL and Extracel-HP is approved by the FDA.
713 Even so, as a whole group, the exact applicability of the
714 current approach needs to be demonstrated. It might utilize
715 a patient's body as a bioreactor to make a tissue engineered
716 graft behave as an autograft to address the limitation of
717 autograft availability and the associated morbidity in their
718 procurement [11]. However, a number of issues must be
719 addressed before this kind of therapeutic strategy can be
720 applied.

721 In the future, BMP-2 loaded hydrogel might be highly
722 active on nearby MSCs if BMP-2 is applied after complete
723 growth of fibro-vascular tissue. Considering the well-
724 established biomaterials and the huge demand of vascular-
725 ized autografts in patients, a well-vascularized engineered
726 bone might satisfy the unmet demand. As a vein graft can be
727 utilized for induction of vascularization, this surgical
728 approach might eventually allow generation of axially
729 vascularized tissues with minimal donor site morbidity
730 independently of anatomic vascular axis.

731 5 Conclusion

732 In this study, we demonstrated that BMP-2 may be con-
733 tained within and slowly released from a Hyaluronan-based
734 hydrogel for more than 5 weeks. The hydrogel along with
735 PLDLLA–TCP–PCL scaffold could be axially vascularized
736 by an A–V loop. The hyaluronan hydrogel was gradually
737 degraded that guided sustained FVT growth and the
738 released BMP-2 induced bone-related gene expression,
739 although the formation of bone could not be observed
740 histologically. Based on the results of this experiment, it
741 can be concluded that the PLDLLA–TCP–PCL-hyaluronan
742 scaffold containing BMP-2 and supplied with an A–V loop
743 can possibly be explored as a well-vascularized bone graft
744 after further optimization.

745 **Acknowledgments** This study was supported by research grants
746 from the Deutsche Forschungsgemeinschaft (DFG) (KN 578/2-1) and
747 the Xue Hong and Hans Georg Geis Foundation. The authors thank
748 Dr. Andreas Hess, Institute of Experimental and Clinical Pharma-
749 cology and Toxicology for helping in micro-CT scanning and Prof.

Peter Greil and Mr. Peter Reinhard for production of the Teflon
chambers.

References

1. Pneumaticos SG, Triantafyllopoulos GK, Basdra EK, Papavasiliou AG. Segmental bone defects: from cellular and molecular pathways to the development of novel biological treatments. *J Cell Mol Med*. 2010. doi:10.1111/j.1582-4934.2010.01062.x. 753
2. Scheufler O, Schaefer DJ, Jaquiere C, Braccini A, Wendt DJ, Gasser JA, et al. Spatial and temporal patterns of bone formation in ectopically pre-fabricated, autologous cell-based engineered bone flaps in rabbits. *J Cell Mol Med*. 2008;12(4):1238–49. doi:10.1111/j.1582-4934.2008.00137.x. 754
3. Arkudas A, Tjiawi J, Bleiziffer O, Grabinger L, Polykandriotis E, Beier JP, et al. Fibrin gel-immobilized VEGF and bFGF efficiently stimulate angiogenesis in the AV loop model. *Mol Med*. 2007;13(9–10):480–7. 755
4. Reddi A. Bone morphogenetic proteins: from basic science to clinical applications. *J Bone Joint Surg J*. 2001;83(Suppl 1, Part 1):S1. 756
5. Arkudas A, Beier J, Heidner K, Tjiawi J, Polykandriotis E, Srour S, et al. Axial prevascularization of porous matrices using an arteriovenous loop promotes survival and differentiation of transplanted autologous osteoblasts. *Tissue Eng*. 2007;13(7):1549–60. 757
6. Kneser U, Schaefer DJ, Polykandriotis E, Horch RE. Tissue engineering of bone: the reconstructive surgeon's point of view. *J Cell Mol Med*. 2006;10(1):7–19. 758
7. Beier J, Horch R, Hess A, Arkudas A, Heinrich J, Loew J, et al. Axial vascularization of a large volume calcium phosphate ceramic bone substitute in the sheep AV loop model. *J Tissue Eng Regen Med*. 2010;4(3):216–23. 759
8. Ai-Aql ZS, Alagl AS, Graves DT, Gerstenfeld LC, Einhorn TA. Molecular mechanisms controlling bone formation during fracture healing and distraction osteogenesis. *J Dent Res*. 2008;87(2):107–18. 760
9. Reddi A. Role of morphogenetic proteins in skeletal tissue engineering and regeneration. *Nat Biotechnol*. 1998;16(3):247–52. 761
10. Eyckmans J, Roberts SJ, Schrooten J, Luyten FP. A clinically relevant model of osteoinduction: a process requiring calcium phosphate and BMP/Wnt signaling. *J Cell Mol Med*. 2009. doi:10.1111/j.1582-4934.2009.00807.x. 762
11. Terheyden H, Menzel C, Wang H, Springer IN, Rueger DR, Acil Y. Prefabrication of vascularized bone grafts using recombinant human osteogenic protein-1—part 3: dosage of rhOP-1, the use of external and internal scaffolds. *Int J Oral Maxillofac Surg*. 2004;33(2):164–72. 763
12. Patel VV, Zhao L, Wong P, Pradhan BB, Bae HW, Kanim L, et al. An in vitro and in vivo analysis of fibrin glue use to control bone morphogenetic protein diffusion and bone morphogenetic protein-stimulated bone growth. *Spine J*. 2006;6(4):397–403. 764
13. Seeherman H, Wozney J, Li R. Bone morphogenetic protein delivery systems. *Spine (Phila Pa 1976)*. 2002;27(16 Suppl 1):S16–23. 765
14. Yamamoto M, Takahashi Y, Tabata Y. Controlled release by biodegradable hydrogels enhances the ectopic bone formation of bone morphogenetic protein. *Biomaterials*. 2003;24(24):4375–83. 766
15. Anitua E, Sánchez M, Orive G, Andia I. Delivering growth factors for therapeutics. *Trends Pharmacol Sci*. 2008;29(1):37–41. 767
16. Meyer R Jr, Gruber H, Howard B, Tabor O Jr, Murakami T, Kwiatkowski T, et al. Safety of recombinant human bone morphogenetic protein-2 after spinal laminectomy in the dog. *Spine*. 1999;24(8):747. 768

- 812 17. Bishop G, Einhorn T. Current and future clinical applications of
813 bone morphogenetic proteins in orthopaedic trauma surgery. *Int*
814 *Orthop*. 2007;31(6):721–7.
- 815 18. Pike DB, Cai S, Pomraning KR, Firpo MA, Fisher RJ, Shu XZ, et al.
816 Heparin-regulated release of growth factors in vitro and angiogenic
817 response in vivo to implanted hyaluronan hydrogels containing
818 VEGF and bFGF. *Biomaterials*. 2006;27(30):5242–51. doi:
819 [10.1016/j.biomaterials.2006.05.018](https://doi.org/10.1016/j.biomaterials.2006.05.018).
- 820 19. Zhao B, Katagiri T, Toyoda H, Takada T, Yanai T, Fukuda T,
821 et al. Heparin potentiates the in vivo ectopic bone formation
822 induced by bone morphogenetic protein-2. *J Biol Chem*. 2006;
823 281(32):23246.
- 824 20. Zein I, Huttmacher DW, Tan KC, Teoh SH. Fused deposition
825 modeling of novel scaffold architectures for tissue engineering
826 applications. *Biomaterials*. 2002;23(4):1169–85.
- 827 21. Lam C, Olkowski R, Swieszkowski W, Tan K, Gibson I,
828 Huttmacher D. Mechanical and in vitro evaluations of composite
829 PLDLLA/TCP scaffolds for bone engineering. *Virtual Phys*
830 *Prototyp*. 2008;3(4):193–7.
- 831 22. Yang J, Wan Y, Tu C, Cai Q, Bei J, Wang S. Enhancing the cell
832 affinity of macroporous poly(L-lactide) cell scaffold by a con-
833 venient surface modification method. *Polym Int*. 2003;52(12):
834 1892–9.
- 835 23. Kneser U, Stangenberg L, Ohnolz J, Buettner O, Stern-Straeter J,
836 Mobest D, et al. Evaluation of processed bovine cancellous bone
837 matrix seeded with syngenic osteoblasts in a critical size calvarial
838 defect rat model. *J Cell Mol Med*. 2006;10(3):695–707.
- 839 24. Kneser U, Polykandriotis E, Ohnolz J, Heidner K, Grabinger L,
840 Euler S, et al. Engineering of vascularized transplantable bone
841 tissues: induction of axial vascularization in an osteoconductive
842 matrix using an arteriovenous loop. *Tissue Eng*. 2006;12(7):
843 1721–31.
- 844 25. Bolland BJRF, Kanczler JM, Dunlop DG, Oreffo ROC. Develop-
845 ment of in vivo μ CT evaluation of neovascularisation in tissue
846 engineered bone constructs. *Bone*. 2008;43(1):195–202.
- 847 26. Arkudas A, Prymachuk G, Hoereth T, Beier J, Polykandriotis E,
848 Bleiziffer O, et al. Dose-Finding Study of Fibrin Gel-Immobi-
849 lized Vascular Endothelial Growth Factor 165 and Basic Fibro-
850 blast Growth Factor in the Arteriovenous Loop Rat Model. *Tissue*
851 *Eng A*. 2009;15(9):2501–11.
- 852 27. Talwar R, Di Silvio L, Hughes FJ, King GN. Effects of carrier
853 release kinetics on bone morphogenetic protein-2-induced peri-
854 odontal regeneration in vivo. *J Clin Periodontol*. 2001;28(4):
855 340–7.
- 856 28. Seeherman H, Li R, Bouxsein M, Kim H, Li X, Smith-Adaline E,
857 et al. rhBMP-2/calcium phosphate matrix accelerates osteotomy-
858 site healing in a nonhuman primate model at multiple treatment
859 times and concentrations. *J Bone Joint Surg*. 2006;88(1):144.
- 860 29. Rothstein S, Federspiel W, Little S. A unified mathematical model
861 for the prediction of controlled release from surface and bulk
862 eroding polymer matrices. *Biomaterials*. 2009;30(8):1657–64.
- 863 30. Adams JR, Sander G, Byers S. Expression of hyaluronan syn-
864 thases and hyaluronidases in the MG63 osteoblast cell line.
865 *Matrix Biol*. 2006;25(1):40–6. doi:[10.1016/j.matbio.2005.08.007](https://doi.org/10.1016/j.matbio.2005.08.007).
- 866 31. Kakudo N, Kusumoto K, Wang YB, Iguchi Y, Ogawa Y. Immu-
867 nocolocalization of vascular endothelial growth factor on intramus-
868 cular ectopic osteoinduction by bone morphogenetic protein-2.
869 *Life Sci*. 2006;79(19):1847–55. doi:[10.1016/j.lfs.2006.06.033](https://doi.org/10.1016/j.lfs.2006.06.033).
- 870 32. Toole BP, Hascall VC. Hyaluronan and tumor growth. *Am J*
871 *Pathol*. 2002;161(3):745–7.
- 872 33. Mazumdar J, Dondeti V, Simon M. Hypoxia-inducible factors in
873 stem cells and cancer. *J Cell Mol Med*. 2009;13(11–12):4319–28.
- 874 34. Jeon O, Song S, Kang S, Putnam A, Kim B. Enhancement of
875 ectopic bone formation by bone morphogenetic protein-2 released
876 from a heparin-conjugated poly(l-lactic-co-glycolic acid) scaf-
877 fold. *Biomaterials*. 2007;28(17):2763–71.
- 878 35. Inoda H, Yamamoto G, Hattori T. rh-BMP2-induced ectopic bone
879 for grafting critical size defects: a preliminary histological eval-
880 uation in rat calvariae. *Int J Oral Maxillofac Surg*. 2007;36(1):
881 39–44.
- 882 36. Murakami T, Saito A, Hino S, Kondo S, Kanemoto S, Chihara K,
883 et al. Signalling mediated by the endoplasmic reticulum stress
884 transducer OASIS is involved in bone formation. *Nat Cell Biol*.
885 2009;11(10):1205–11. doi:[10.1038/ncb1963](https://doi.org/10.1038/ncb1963).
- 886 37. Lamoureux F, Baud'huin M, Duplomb L, Heymann D, Redini F.
887 Proteoglycans: key partners in bone cell biology. *BioEssays*.
888 2007;29(8).
889